$E0$ components of $2_i^+ \rightarrow 2_f^+$ transitions in even cadmium isotopes and effective monopole charges

A. Giannatiempo, A. Nannini, A. Perego, and P. Sona
Dipartimento di Fisica and Istituto Nazionale di Fisica Nucleare, Florence, Italy
(Received 26 July 1991)

The K-internal conversion coefficients of the $2_2^+ \rightarrow 2_1^+$ and $2_3^+ \rightarrow 2_1^+$ transitions in ^{110}Cd and the $2_3^+ \rightarrow 2_1^+$ transition in ^{112}Cd have been measured. The available experimental information on K-conversion coefficients, mixing ratios $E2/M1$, and lifetimes for the $2_i^+ \rightarrow 2_f^+$ transitions in ^{110,112,114}Cd have been utilized to deduce the ratios $B(E0)/B(E2)$, and $B(E0)/B(M1)$ and the monopole strength parameter ρ^2. The experimental data are compared to the theoretical values calculated in the framework of the interacting proton-neutron boson model. By exploiting also the available data on ρ^2 for the $0_2^+ \rightarrow 0_1^+$ transitions in these nuclei the boson effective charges in the $E0$ operator have been deduced.

INTRODUCTION

The excitation pattern of low-lying levels in ^{110,112,114}Cd resembles that of a harmonic vibrator were it not for the presence of two additional states having $J^\pi = 2^+, 0^+$ at energies close to the two-phonon triplet. According to the usual interpretation given in the literature [1–4], these "intruder" states are due to the excitation of two protons across the $Z=50$ closed shell.

We have recently analyzed [5] excitation energies, quadrupole moments and transitions, magnetic dipole moments, and $E2/M1$ mixing ratios for the low-lying levels of ^{110,112,114}Cd in the framework of the interacting boson model (IBA-2). With the exception of the 0_3^+ state, a reasonable overall agreement between the observed and the predicted properties was obtained. In particular, it was possible to interpret the 2_3^+ state as a rather pure $F = F_{\max} - 1$ ("mixed-symmetry") state and it was not necessary to invoke additional configurations outside the IBA-2 space.

In the present work we report on the measurement of the K-conversion coefficient α_K of some $2_i^+ \rightarrow 2_f^+$ transitions in ^{110}Cd and in ^{112}Cd performed with the aim of deducing their $E0$ component. This new information, together with data already available in the literature, is then used to extend our previous analysis to $E0$ transitions in these nuclei.

EXPERIMENTAL PROCEDURE AND RESULTS

In this work, the K conversion coefficients of the $2_3^+ \rightarrow 2_1^+$, 851-keV transition in ^{112}Cd and the $2_2^+ \rightarrow 2_1^+$, 818-keV and $2_3^+ \rightarrow 2_1^+$, 1125-keV transitions in ^{110}Cd have been measured. The levels of interest in ^{110,112}Cd were populated via the β^+ decay of ^{110}In ($T_{1/2} = 69$ min) and ^{112}In ($T_{1/2} = 14.4$ min) produced via the (p,n) reaction at Laboratori Nazionali di Legnaro (Padua) using the proton beam from the CN Van de Graaff accelerator at an energy of 6.8 MeV. Typical beam currents were in the range 1.5–1.8 μA. The targets were produced by vacuum deposition of ^{110}Cd (93% enriched) and ^{112}Cd (94% enriched) on a thick carbon backing and were cooled down to liquid-nitrogen temperature so as to avoid the damage from excessive heat loading during irradiation. Bombarding and measuring periods (separated by a waiting period of proper length to allow the decay of short-lived activities) were alternated under computer control.

Energy spectra of gamma rays and internal conversion electrons were simultaneously recorded using a multiplexed acquisition system. Gamma rays were detected by means of a HP Ge detector having a resolution (FWHM) of 2.5 keV at 1.33 MeV. Conversion electrons were analyzed by means of a magnetic transport system (described in detail in Ref. [6]) followed by a 5-mm-thick Si(Li) detector cooled to liquid-nitrogen temperature. It had an energy resolution of about 2.4 keV at an energy of 1 MeV. To correct for different dead-time losses in the gamma and electron acquisition channels, the signals from a high-stability pulser at a frequency of 1 Hz were routed (slightly shifted in time) to the preamplifier inputs. For each K-conversion line of interest, the transport system was employed with a magnetic-field setting corresponding to its maximum transmission. The proportionality constant relating the selected electron momentum to the magnetic field has to be calibrated for each run as it depends on the position of the beam spot on the target. To this purpose, the maximum transmission was determined for the K-conversion electrons of the very intense $2_1^+ \rightarrow 0_1^+$, 657-keV transition in ^{110}Cd by scanning the transmission curve over a range of magnetic-field settings. The relevant sections of the electron energy spectra recorded for the transitions of interest are reported in Figs. 1(a)–1(d).

To evaluate the integrals I_K of the K-conversion lines, which have an asymmetric shape, the peaks in the energy spectra were fitted by a function resulting from the convolution of a Gaussian curve with a delta function plus an exponential "tail" on the low-energy side. The background was simultaneously fitted by a second-order polynomial so that, altogether, an eight-parameter fit was performed for each line. In the particular case of the 818.0-keV transition in ^{110}Cd, the evaluation of the peak area was complicated by the presence of the $0_2^+ \rightarrow 2_1^+$, 815.4-keV line [see Fig. 1(b)]. However, the fitting procedure could give an accurate value of both peak areas as confirmed by the deduced K-conversion coefficient of the

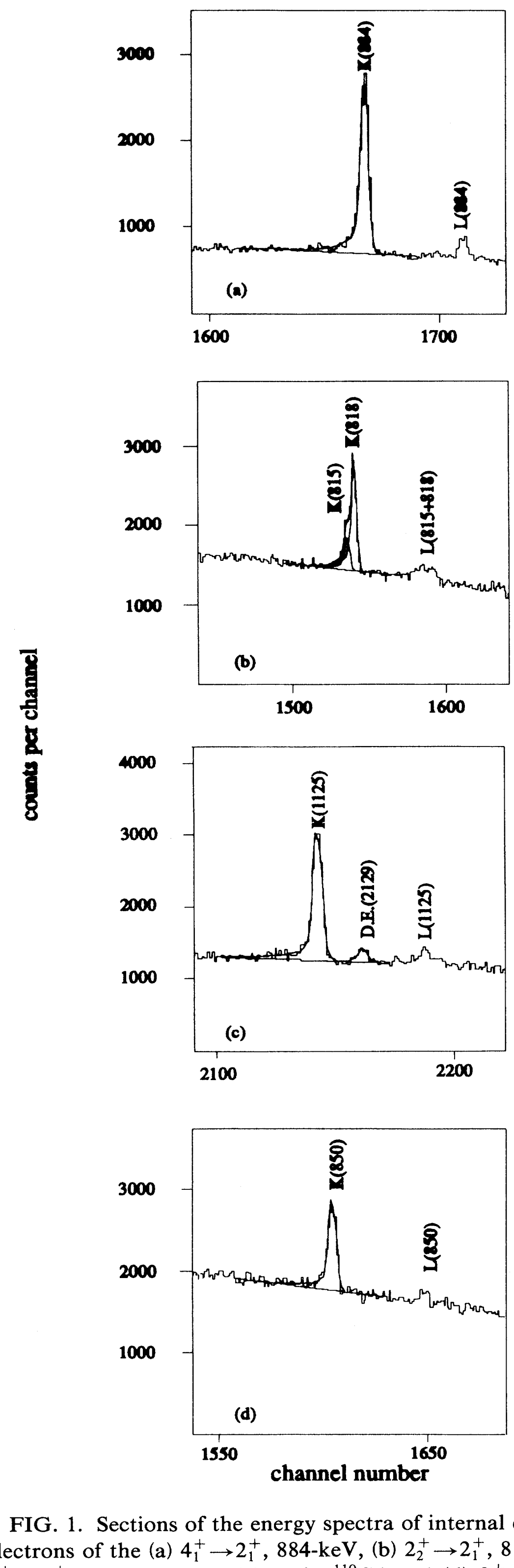

FIG. 1. Sections of the energy spectra of internal conversion electrons of the (a) $4_1^+ \to 2_1^+$, 884-keV, (b) $2_2^+ \to 2_1^+$, 818-keV, (c) $2_3^+ \to 2_1^+$, 1125-keV transitions in ^{110}Cd and (d) $2_3^+ \to 2_1^+$, 850-keV transition in ^{112}Cd. The doublet in (b) is due to the presence of the $0_2^+ \to 2_1^+$, 815-keV transition in ^{110}Cd. In (c), the label DE refers to the double escape peak of the 2129-keV γ ray in ^{110}Cd.

815 keV transition which is in good agreement with the theoretical value [7] for a pure $E2$ transition.

For the areas I_γ under the peaks in the gamma energy spectra, a simple fit with a Gaussian curve plus a linear background proved to be satisfactory.

The K-conversion coefficients were determined by means of the normalized peak to gamma method (NPG) method [8], which consists in normalizing the relative conversion electron and gamma-ray intensity via the corresponding intensity of a transition of known conversion coefficient.

The expression of the experimental K-conversion coefficient α_K^{expt} is given by

$$\alpha_K^{\text{expt}}(E) = \frac{I_K(E)}{I_K(E_R)} \frac{\eta_e(E_R)}{\eta_e(E)} \frac{I_\gamma(E_R)}{I_\gamma(E)} \frac{\eta_\gamma(E)}{\eta_\gamma(E_R)} \alpha_K(E_R) , \tag{1}$$

where η_γ and η_e are the full energy peak efficiencies for gamma and electrons at the energy of interest E and at the energy E_R of the reference line and $\alpha_K(E_R)$ is the theoretical conversion coefficient of the reference line. It is seen that only relative detection efficiencies are needed. These were determined in the usual way by placing suitable electron and gamma sources at the target position.

The $4_1^+ \to 2_1^+$, 884-keV transition in ^{110}Cd, which has pure $E2$ multipolarity and an energy close to that of the transitions of interest, has been taken as the reference line. To have a check of the whole procedure, we evaluated the K-conversion coefficient of the $2_1^+ \to 0_1^+$, 657-keV transition in ^{110}Cd and found a value differing from the theoretical one [7] by less than 1%.

The procedure whereby information on the $E0$ component of a transition between two states having the same $J^\pi \neq 0$ can be extracted is based on the comparison between the measured value α_K^{expt} and the value corresponding to a transition having $E0$, $M1$, and $E2$ multipole components, according to the expression

$$\alpha_K^{\text{expt}} = \frac{\alpha_K^{\text{th}}(M1) + (1+q^2)\delta^2 \alpha_K^{\text{th}}(E2)}{(1+\delta^2)} . \tag{2}$$

Here $\alpha_K^{\text{th}}(E2)$ and $\alpha_K^{\text{th}}(M1)$ are theoretical K-conversion coefficients and q^2 is the intensity ratio $W_K(E0)/W_K(E2)$ of the K-conversion electrons for the monopole and quadrupole components.

For small values of δ^2 we found it convenient to express the dependence of α_K^{expt} on the $E0$ component through the ratio $p^2 = W_K(E0)/W_K(M1)$ according to the expression

$$\alpha_K^{\text{expt}} = \frac{\alpha_K^{\text{th}}(M1)(1+p^2) + \alpha_K^{\text{th}}(E2)\delta^2}{(1+\delta^2)} . \tag{3}$$

If the square of the mixing ratio δ^2 is known, q^2 and p^2 can be deduced.

One can then derive the ratio of the reduced transition probabilities $B(E0)/B(E2)$ through the relation [9]

$$B(E0; J_i^+ \to J_f^+)/B(E2; J_i^+ \to J_f^+)$$
$$= 2.56 \times 10^9 A^{4/3} E_\gamma^5 [\text{MeV}] \frac{\alpha_K(E2)}{\Omega_K[s^{-1}]} q^2 \tag{4}$$

and the ratio $B(E0)/B(M1)$ through the relation

$$B(E0;J_i^+\to J_f^+)/B(M1;J_i^+\to J_f^+)=2.07\times10^{13}A^{4/3}E_\gamma^3[\mathrm{MeV}]\frac{\alpha_K(M1)}{\Omega_K[s^{-1}]}p^2 . \quad (5)$$

In (4) and (5), Ω_K is the "electronic" factor for the K conversion of the $E0$ transition. In (5), $B(E0)/B(M1)$ is given in units of $e^2\,\mathrm{fm}^4\mu_N^{-2}$.

Finally, if the $E2$ gamma transition probability $W_\gamma(E2)$ is known, one can deduce the monopole strength parameter ρ^2 which is related to q^2 by the expression [9]

$$\rho^2(E0;J_i^+\to J_f^+)=\frac{\alpha_K(E2)W_\gamma(E2;J_i^+\to J_f^+)}{\Omega_K}q^2 . \quad (6)$$

Our experimental results on the K-conversion coefficients together with those available on the $2_i^+\to2_f^+$ transitions in ^{110,112,114}Cd are reported in Table I together with the corresponding δ^2. The intensity ratios q^2 and p^2 (given in columns 8 and 9) have been deduced from (2) and (3) using for Ω_K and α_K^{th} the values taken from Refs. [10] and [7].

It is to be noted that the relative errors on p^2 are smaller or greater than the relative errors on q^2 according to whether $\delta^2<1$ or $\delta^2>1$.

We remark that, in the presence of penetration effects [11], $\alpha_K^{\mathrm{th}}(M1)$ in (2) and (3) is to be replaced by $\alpha_K^{\mathrm{th}}(M1)(1+B_{1K}\lambda+B_{2K}\lambda^2)$, where λ is the penetration parameter and B_{iK} are the penetration coefficients tabulated in Ref. [12]. We have evaluated the correction factor $(1+B_{1K}\lambda+B_{2K}\lambda^2)$ for $\lambda=\pm5$ (which seems to be a reasonable limit for these nuclei [13–15] also considering the hindrance factors of the $M1$ components) and found that the variations in the calculated value of q^2 (hence of ρ^2) are significantly smaller than the quoted errors. For what concerns p^2, the variation is usually negligible except for two cases in which it is of the order of the quoted errors.

We observe that the only missing experimental value necessary to complete the information on the transitions among the three lowest 2^+ states in these nuclei is the value of α_K^{expt} for the $2_2^+\to2_1^+$ transition in ^{112}Cd. In our particular case, we could not determine an accurate enough value of α_K^{expt} due to the very weak population of the 2_2^+ level from the ^{112}In decay [16].

The deduced values of $B(E0)/B(E2)$, $B(E0)/B(M1)$, and ρ^2 are reported in Table II. We remark that the ratio $B(E0)/B(M1)$ for the $2_3^+\to2_1^+$ transitions rapidly increases in going from ^{110}Cd to ^{114}Cd.

DISCUSSION

The interpretation of $E0$ transitions is still plagued by several difficulties owing to the generally complicated nature of some excited 0^+ states as well as to the scarcity and limited precision of the experimental data which, in turn, makes it difficult to determine the relevant parameters (effective monopole charges) appearing in the theoretical models. In this work we have performed an analysis of the available experimental data on $E0$ transitions between the low-lying levels in ^{110,112,114}Cd in the framework of the IBA-2 model.

In this model the $E0$, $M1$, and $E2$ transition operators have the expressions [17]

$$\hat{T}(E0)=\beta_{0\nu}\hat{T}_\nu(E0)+\beta_{0\pi}\hat{T}_\pi(E0)=\beta_{0\nu}(d_\nu^\dagger\times\tilde{d}_\nu)^{(0)}+\beta_{0\pi}(d_\pi^\dagger\times\tilde{d}_\pi)^{(0)} , \quad (7)$$

$$\hat{T}(M1)=g_\nu\hat{T}_\nu(M1)+g_\pi\hat{T}_\pi(M1)=\sqrt{30/4\pi}[g_\nu(d_\nu^\dagger\times\tilde{d}_\nu)^{(1)}+g_\pi(d_\pi^\dagger\times\tilde{d}_\pi)^{(1)}] , \quad (8)$$

$$\hat{T}(E2)=e_\nu\hat{Q}_\nu+e_\pi\hat{Q}_\pi , \quad (9)$$

$$\hat{Q}_\rho=[d_\rho^\dagger\times\tilde{s}_\rho+s_\rho^\dagger\times\tilde{d}_\rho]^{(2)}+\chi_\rho[d_\rho^\dagger\times\tilde{d}_\rho]^{(2)} , \quad (10)$$

where the indexes ν and π refer to neutron and proton bosons, respectively. The parameters $\beta_{0\rho}$ and e_ρ are the effective monopole and quadrupole charges and g_ρ the effective g factors ($\rho=\nu,\pi$).

TABLE I. Experimental results on α_K values measured in this work and on available α_K of the $2_i^+\to2_f^+$ transitions in ^{110,112,114}Cd are reported in columns 3 and 4. In the following columns (5–7), the corresponding theoretical values for the $E2$ and $M1$ transitions and the available experimental data on δ^2 are given. In the last two columns are reported the intensity ratios q^2 and p^2 derived from (2) and (3). The indicated upper limits of q^2 and p^2 for the $2_2^+\to2_1^+$ transition in ^{114}Cd are at the 99% confidence level.

A	$J_i^\pi\to J_f^\pi$	$10^3\alpha_K$ Experiment Present work	Previous work	Theory[d] $E2$	$M1$	δ^2	q^2	p^2
110	$2_2^+\to2_1^+$	1.74(9)	1.84(12)[a]	1.59	1.86	1.85(19)[a]	0.09(7)	0.15(11)
114	$2_2^+\to2_1^+$		2.69(17)[b]	2.80	3.15	1.49(73)[b]	≤0.18	≤0.22
110	$2_3^+\to2_1^+$	0.95(5)	0.90(20)[a]	0.772	0.909	0.014(28)[e]	4.6(9.8)	0.055(53)
112	$2_3^+\to2_1^+$	2.34(12)		1.44	1.69	0.048(22)[f]	9.9(4.6)	0.41(7)
114	$2_3^+\to2_1^+$		3.66(24)[c]	1.65	1.92	0.0023(20)[g]	392(309)	0.91(12)
114	$2_3^+\to2_2^+$		434(39)[c]	257	121	$3.8_{-1.3}^{+0.3}$[h]	$1.01_{-0.19}^{+0.22}$	$8.1_{-1.6}^{+2.4}$

[a]Reference [21].
[b]Reference [22].
[c]Average from Refs. [23] and [24].
[d]Reference [7].
[e]Reference [25].
[f]Reference [16].
[g]Reference average from Refs. [26]–[28].
[h]Reference [24].

TABLE II. The experimental values of $B(E0)/B(E2)$, $B(E0)/B(M1)$, and ρ^2 in ^{110,112,114}Cd are compared to the theoretical ones evaluated using for the parameters of the $E0$, $E2$, and $M1$ operators the values $\beta_{0\nu}=0.25$ e fm^2, $\beta_{0\pi}=0.1$ e fm^2, $e_\nu=8.7$ e fm^2, $e_\pi=10.5$ e fm^2, $g_\nu=0.21\mu_N$, $g_\pi=0.55\mu_N$. Values reported in columns 3 and 4 for $0_2^+\rightarrow 0_1^+$ transitions refer to the ratio $B(E0;0_2^+\rightarrow 0_1^+)/B(E2;0_2^+\rightarrow 2_1^+)$. The ratio $B(E0)/B(M1)$ is given in units of e^2fm$^4\mu_N^{-2}$. The experimental values of ρ^2 given in column 7 are deduced according to (6) of the text utilizing, for $W_\gamma(E2)$, the data in Refs. [21], [16], and [22].

A	$J_i^+\rightarrow J_f^+$	$B(E0)/B(E2)$ Experiment	$B(E0)/B(E2)$ Theory	$B(E0)/B(M1)$ Experiment	$B(E0)/B(M1)$ Theory	$\rho^2(E0)$ Experiment Present work	$\rho^2(E0)$ Experiment Previous work	$\rho^2(E0)$ Theory
110	$2_2^+\rightarrow 2_1^+$	0.023(17)[a]	0.008	923(680)[a]	2.8×10^4	0.020(15)[a]		0.005
114	$2_2^+\rightarrow 2_1^+$	≤ 0.035	0.009	≤ 1471	3.3×10^4	≤ 0.028	≤ 0.008[e]	0.007
110	$2_3^+\rightarrow 2_1^+$	1.9 ± 4.1	2.9	304(294)	970			0.024
112	$2_3^+\rightarrow 2_1^+$	2.7 ± 1.3	4.5	2555(472)	1340	0.031(20)		0.033
114	$2_3^+\rightarrow 2_1^+$	100 ± 79	3.6	5938(820)	1880	$0.113^{+0.093}_{-0.108}$	0.061,[e] ≥ 0.350[f]	0.041
114	$2_3^+\rightarrow 2_2^+$	$0.032^{+0.007}_{-0.006}$	0.036	$(7.3^{+1.4}_{-2.2})\times 10^4$	55×10^4	0.028(9)	0.034[e]	0.007
110	$0_2^+\rightarrow 0_1^+,2_1^+$	0.027(4)[b]	0.032					0.029
112	$0_2^+\rightarrow 0_1^+,2_1^+$	0.025(3)[c]	0.028				0.037(11)[d]	0.029
114	$0_2^+\rightarrow 0_1^+,2_1^+$	0.025(8)[d]	0.033				0.030(8)[d]	0.035

[a]Obtained using for α_K the weighted average of the two experimental data.
[b]Reference [29].
[c]Reference [30].
[d]Reference [31].
[e]Reference [1].
[f]Reference [26].

The $E0$ transition matrix element ρ is defined [18] as

$$\rho(E0;J_i^+\rightarrow J_f^+)=\frac{Z}{eR^2}[\beta_{0\nu}\langle J_f|\hat{T}_\nu(E0)|J_i\rangle + \beta_{0\pi}\langle J_f|\hat{T}_\pi(E0)|J_i\rangle]\ , \quad (11)$$

where $R=1.2A^{1/3}$fm. The parameters $\beta_{0\pi}$ and $\beta_{0\nu}$ are to be expressed in e fm^2. The reduced monopole transition probability $B(E0)$ is related to the monopole strength parameter ρ^2 by the expression

$$B(E0)=\rho^2(E0)e^2R^4\ . \quad (12)$$

The calculations have been performed with the Hamiltonian parameters deduced in [5] from a global analysis of the experimental data concerning excitation energies and $E2$ and $M1$ matrix elements of low-lying levels in ^{110,112,114}Cd, with the exception of those relative to the 0_3^+ level whose description possibly requires an extension of the model. We used the code NPBOS [19].

To evaluate the parameters of the $E0$ operator, a comparison of the six experimental data on ρ^2 given in Table II with the corresponding theoretical values was performed by computing the standard expression of χ^2 for values of $\beta_{0\nu}$ and $\beta_{0\pi}$ in the range $[-2,2]$ e fm^2. The results are summarized in Fig. 2 in the form of a contour plot for the normalized χ^2. There are two broad minima centered at about the values $\beta_{0\nu}=0.25$ e fm^2, $\beta_{0\pi}=0.1$ e fm^2 and $\beta_{0\nu}=0.1$ e fm^2, $\beta_{0\pi}=0.6$ e fm^2. Obviously, the same minima would be obtained if both $\beta_{0\nu}$ and $\beta_{0\pi}$ were reversed in sign which, however, seems to be unphysical.

By using the values $\beta_{0\nu}=0.25$ e fm^2, $\beta_{0\pi}=0.1$ e fm^2, which correspond to the deeper minimum, and the values of the $E2$ effective charges and g factors determined in Ref. [5], we have calculated the theoretical values for the quantities $B(E0)/B(E2)$, $B(E0)/B(M1)$, and ρ^2. They are reported in Table II. First of all we note that the values of ρ^2 are well reproduced with the only exception of that corresponding to the $2_3^+\rightarrow 2_2^+$ transition in ^{114}Cd.

For what concerns the ratios $B(E0)/B(M1)$, we observe that those corresponding to the $2_2^+\rightarrow 2_1^+$ transitions are grossly overestimated while those relative to the $2_3^+\rightarrow 2_1^+$ transitions are somewhat closer to the experimental values and reproduce the increasing trend in going from ^{110}Cd to ^{114}Cd.

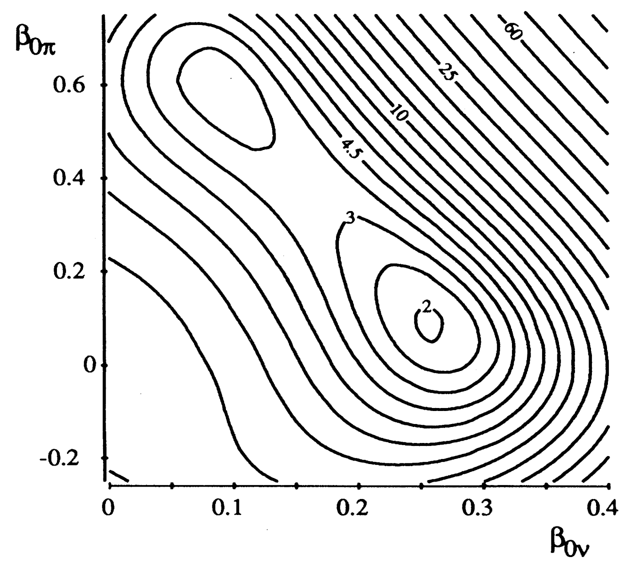

FIG. 2. Contour plot for the variable χ_2 derived from a comparison of theoretical and experimental values of ρ^2 values as a function of the boson effective monopole charges $\beta_{0\pi}$ and $\beta_{0\nu}$ (in units of e fm^2).

TABLE III. The intensity (amplitude square) of the $F=F_{max}$ component in the wave functions of the indicated levels is given in columns 3 and 5. In the last three columns the matrix elements for the neutron and proton part of the electric monopole and magnetic dipole transition operators are reported. The matrix elements of the $\hat{T}_\pi(M1)$ operator are not reported since they have the same absolute value and opposite sign with respect to those of $\hat{T}_\nu(M1)$.

A	J_i^π	$I(F_{max})$	J_f^π	$I(F_{max})$	$\langle \hat{T}_\nu(E0) \rangle$	$\langle \hat{T}_\pi(E0) \rangle$	$\langle \hat{T}_\nu(M1) \rangle$
110	2_2^+	0.97	2_1^+	0.93	0.364	0.224	-0.102
112	2_2^+	0.95	2_1^+	0.90	0.479	0.195	-0.076
114	2_2^+	0.94	2_1^+	0.87	0.452	0.215	-0.117
110	2_3^+	0.13	2_1^+	0.93	1.245	-0.736	1.085
112	2_3^+	0.21	2_1^+	0.90	1.406	-0.689	1.075
114	2_3^+	0.26	2_1^+	0.87	1.529	-0.615	1.036

For the sake of clarifying how this trend can arise, we recall that, in the IBA-2 model, states having full symmetry in neutron and proton degrees of freedom are characterized by the F-spin [17] value $F=F_{max}=N/2$ ($N=$total number of bosons) while the lowest states having mixed symmetry are characterized by $F=F_{max}-1$. In the U(5) limit (which corresponds in a geometrical picture to a vibrational nucleus), the first mixed-symmetry state has $J^\pi=2^+$. In this limit, the F spin is a good quantum number and this implies that the neutron and proton part of the matrix element of an operator $\hat{T}$ between states with different F-spin values must have the same magnitude and opposite sign [20]. In Ref. [5] we found that the 2_3^+ state in ^{110,112,114}Cd is probably to be identified as the lowest mixed-symmetry state, while the 2_1^+ and 2_2^+ states turned out to be of quite pure full symmetry character. This reflects into the presently calculated values of $\langle \hat{T}_\nu(E0) \rangle$ and $\langle \hat{T}_\pi(E0) \rangle$having opposite sign for the $2_3^+ \rightarrow 2_1^+$ transitions and the same sign for the $2_2^+ \rightarrow 2_1^+$ transitions. Their values are reported in Table III together with that of the matrix element $\langle \hat{T}_\nu(M1) \rangle$.

In going from ^{110}Cd to ^{114}Cd, one moves away from the U(5) limit as seen from the variation of the intensity of the $F=F_{max}$ component in the wave functions of the levels reported in Table III. Correspondingly, the difference between the absolute values of $\langle \hat{T}_\nu(E0) \rangle$ and $\langle \hat{T}_\pi(E0) \rangle$ increases for the $2_3^+ \rightarrow 2_1^+$ transitions. The observed increasing trend of $B(E0)/B(M1)$ then follows, given the effective charges determined above and the slight decrease of the $B(M1)$ values. No such trend is present in the calculated values of the monopole component of the $2_2^+ \rightarrow 2_1^+$ transitions due to the fact that $\langle \hat{T}_\nu(E0) \rangle$ and $\langle \hat{T}_\pi(E0) \rangle$ have the same sign. The large overestimate of the ratio $B(E0)/B(M1)$ for these transitions is probably to be ascribed to the well-known difficulty of the IBA-2 model in reproducing $M1$ transition strengths between full symmetry states as already seen, for example, in Ref. [5], where the δ values of the $2_2^+ \rightarrow 2_1^+$ transitions have been also grossly overestimated. This statement is also supported by the agreement between theoretical and experimental values of the ratios $B(E0)/B(E2)$ (see Table II).

CONCLUSIONS

In this work we have reported on the measurement of the K-conversion coefficients of the $2_2^+ \rightarrow 2_1^+$ transitions in ^{112}Cd and $2_2^+ \rightarrow 2_1^+$, $2_3^+ \rightarrow 2_1^+$ transitions in ^{110}Cd. These data complete the systematics of K- conversion coefficients of transitions between low-lying 2^+ states in ^{110,112,114}Cd, with the only exception of the $2_2^+ \rightarrow 2_1^+$ transition in ^{112}Cd. This new information together with that already available in the literature is utilized to estimate the ratios $B(E0)/B(E2)$ and $B(E0)/B(M1)$ and the monopole strength parameter ρ^2 for these transitions. We have compared the deduced values of ρ^2, as well as those available for the $0_2^+ \rightarrow 0_1^+$ transitions in ^{112,114}Cd, with those calculated in the framework of the IBA-2 model to extract the parameters $\beta_{0\nu}$ and $\beta_{0\pi}$ of the $E0$ operator. The observed trend of the ratio $B(E0)/B(M1)$ for the $2_3^+ \rightarrow 2_1^+$ transitions supports the interpretation of the 2_3^+ level as the first mixed-symmetry state in these nuclei.

We are grateful to Dr. G. Maino for many useful discussions, to I. Motti for his assistance in operating the accelerator, and to Dr. P. del Carmine, M. Ottanelli, and A. Pecchioli for their essential technical assistance.

[1] K. Heyde, P. van Isacker, M. Waroquier, G. Wenes, and M. Sambataro, Phys. Rev. C **25**, 3160 (1982).
[2] M. Sambataro, Nucl. Phys. **A380**, 365 (1982).
[3] K. Heyde, P. van Isacker, R. F. Casten, and J. L. Wood, Phys. Lett. **155B**, 303 (1985).
[4] K. Schreckenbach *et al.*, Phys. Lett. **110B**, 364 (1982).
[5] A. Giannatiempo, A. Nannini, A. Perego, and P. Sona, Phys. Rev. C **44**, 1508 (1991).
[6] T. Fazzini, A. Giannatiempo, and A. Perego, Nucl. Instrum. Methods, **211**, 125 (1983).
[7] F. Rösel, H. M. Fries, K. Alder, and H. C. Pauli, At. Data Nucl. Data Tables **21**, 91 (1978).
[8] H. C. Pauli, K. Alder, and R. M. Steffen, in *The Electromagnetic Interaction in Nuclear Spectroscopy,* edited by W. D. Hamilton (North-Holland, Amsterdam, 1975), p. 451.

[9] A. V. Alduschenkov and N. A. Voinova, Nucl. Data Tables **11**, 299 (1973).
[10] D. A. Bell, C. E. Alvedo, M. G. Davidson, and J. P. Davidson, Can. J. Phys. **48**, 2542 (1970).
[11] E. L. Church and J. Weneser, Annu. Rev. Nucl. Sci. **10**, 193 (1960).
[12] R. S. Hager and E. C. Seltzer, Nucl. Data Tables **6**, 1 (1969).
[13] A. Giannatiempo, A. Perego, and P. Sona, Nuovo Cimento A **70**, 15 (1982).
[14] A. Giannatiempo, A. Perego, and P. Sona, Z. Phys. A **306**, 57 (1982).
[15] A. Giannatiempo, A. Perego, and P. Sona, Z. Phys. A **319**, 153 (1984).
[16] D. De Frenne, E. Jacobs, and M. Verboven, Nucl. Data Sheets **57**, 443 (1989).
[17] F. Iachello and A. Arima, *The Interacting Boson Model* (Cambridge University, Cambridge, 1987).
[18] R. Bijker, A. E. Dieperink, and O. Scholten, Nucl. Phys. **A344**, 207 (1980).
[19] T. Otsuka and N. Yoshida, Program NPBOS, Japan Atomic Energy Research Institute Report JAERI-M85-094, 1985.
[20] P. van Isacker, K. Heyde, J. Jolie, and A. Sevrin, Ann. Phys. **171**, 253 (1986).
[21] P. de Gelder, E. Jacobs, and D. De Frenne, Nucl. Data Sheets, **38**, 548 (1983).
[22] J. Blanchot and G. Marguier, Nucl. Data Sheets **60**, 139 (1983).
[23] A. Bäcklin, N. E. Holmberg, and G. Bäckström, Nucl. Phys. **80**, 154 (1966).
[24] A. Mheemeed *et al.*, Nucl Phys. **A412**, 113 (1984).
[25] J. Lange, Krishna Kumar, and J. H. Hamilton, Rev. Mod. Phys. **54**, 119 (1982).
[26] P. Hungerford and W. D. Hamilton, J. Phys. G. **8**, 1107 (1982).
[27] C. Fahlander *et al.*, Nucl. Phys. **A485**, 327 (1988).
[28] S. Yu. Araddad, A. M. Demidov, O. K. Zhuravlev, S. M. Zlitni, V. A. Kurkin, and Dzh. M. Rateb, Yad. Fiz. **46**, 40 (1987) [Sov. J. Nucl. Phys. **46**, 25 (1987)].
[29] A. Giannatiempo, A. Nannini, A. Perego, and P. Sona, Phys. Rev. C **41**, 1167 (1990).
[30] A. Giannatiempo, G. Liberati, and P. Sona, Z. Phys. A **290**, 411 (1979).
[31] R. Julin, J. Kantele, M. Luontama, A. Passoja, T. Poikolainen, A. Bäckin, and N. G. Jonsson, Z. Phys. A **296**, 315 (1980).